



Supplement of

El Niño meets elevated Tibetan Plateau snow cover: independent and synergistic effects on the winter PM_{2.5} dipole pattern in China

Xiaorui Zhang et al.

Correspondence to: Meng Gao (mmgao2@hkbu.edu.hk)

The copyright of individual parts of the supplement might differ from the article licence.

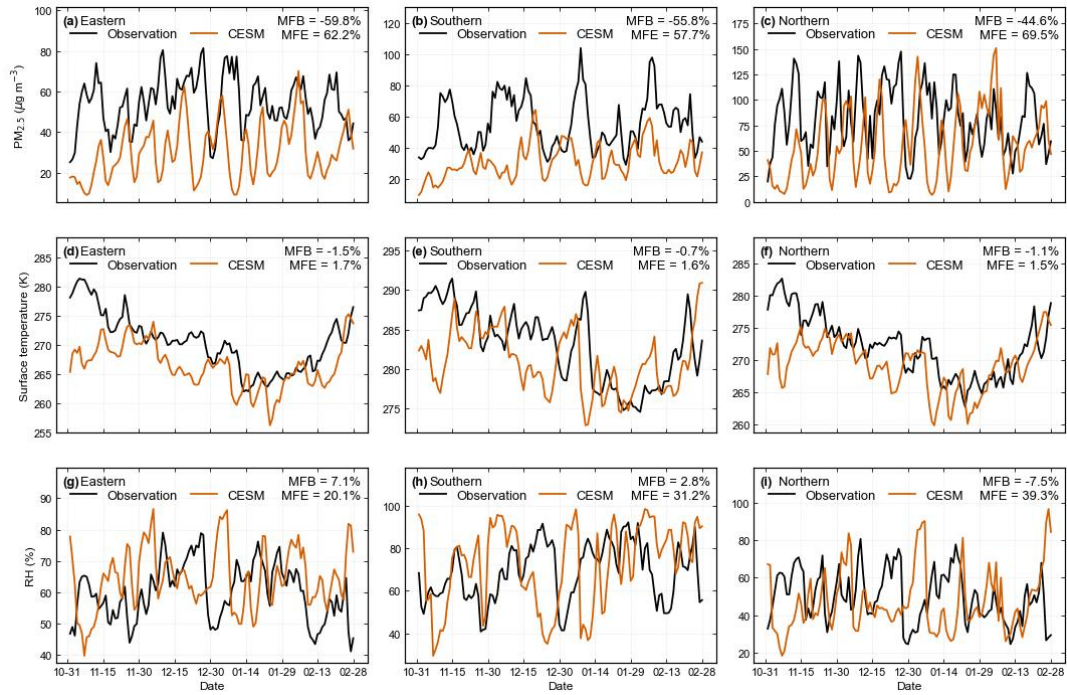


Figure S1. Model evaluation of the CESM_{ctrl}. Simulated and observed daily (a-c) surface PM_{2.5} concentration ($\mu\text{g m}^{-3}$), (d-f) surface air temperature (K), (g-i) relative humidity (%) over eastern China (110° - 135°E , 15° - 50°N), southern China (110° - 135°E , 15° - 30°N) and northern China (110° - 135°E , 35° - 50°N), during November 2010 to February 2011. The mean fractional biases (MFBs) and the mean fractional errors (MFEs) of all simulations meet the model performance criteria of within ± 0.6 for MFB and less than $+ 0.75$ for MFE.

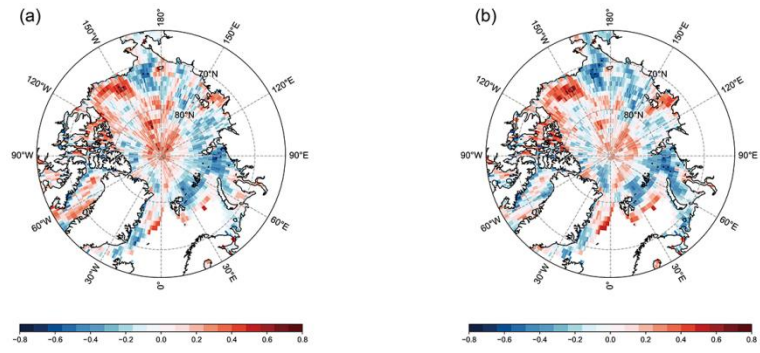


Figure S2. (a) Correlation and (b) partial correlation patterns of PC2 with Arctic sea ice, with the influence of Niño 1+2 removed. Dotted areas represent statistical significance with 95% confidence according to Student's *t* test.

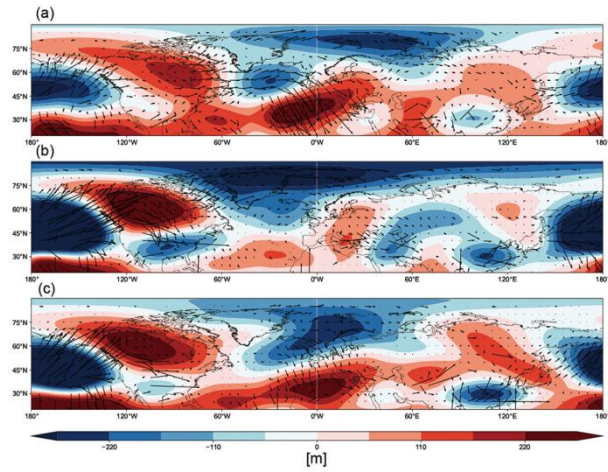


Figure S3. Regression of geopotential height (m) and corresponding wave activity flux (vectors) at 200 hPa during winter from 2005 to 2021 on (a) PC2, (b) Niño 1+2 and (c) Niño 3.4.

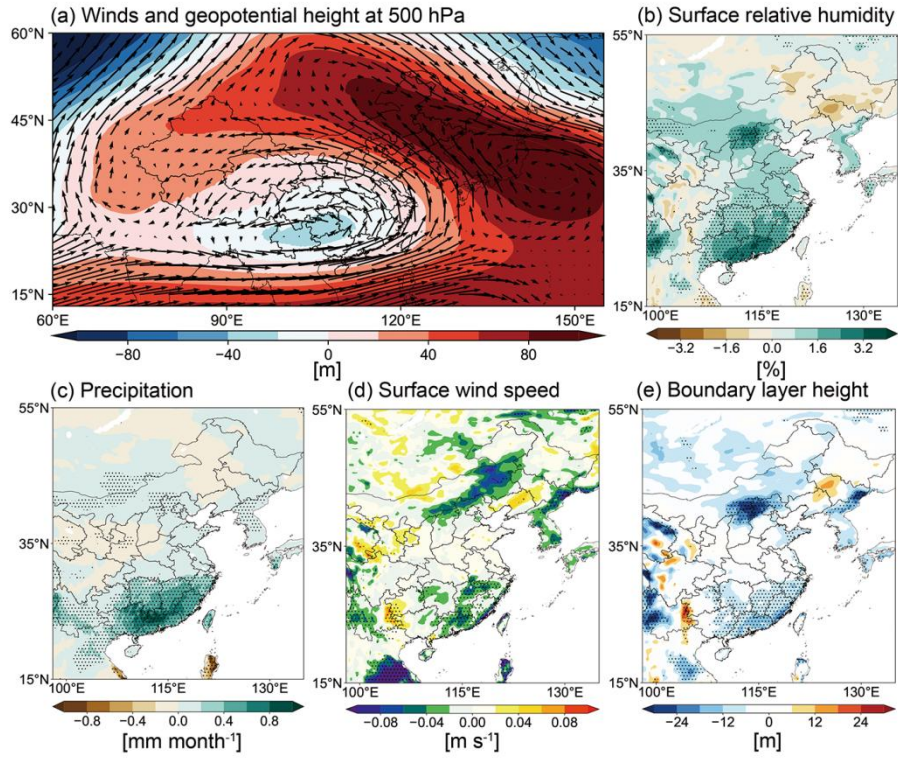


Figure S4. Anomalies for (a) geopotential height (m, shading) and wind fields (m s^{-1} , vector) at 500 hPa, (b) relative humidity at 1000 hPa (%), (c) total precipitation (mm month^{-1}), (d) surface wind speed (m s^{-1}), and (e) planetary boundary layer height (m) during winter over 1979-2021 obtained by regression upon normalized Niño 3.4 index. Dotted areas represent statistical significance with 95% confidence according to Student's *t* test.

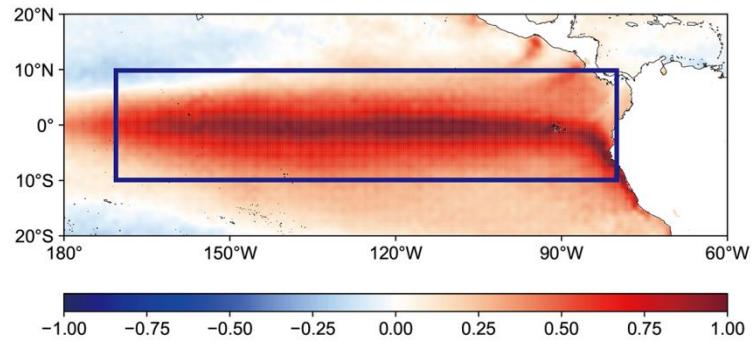


Figure S5. Composite difference of winter averaged sea surface temperature (K) between positive Niño 1+2 years and climatological mean over 1979-2021 (The blue box represent the region with sea surface temperature anomaly imposed in Community Earth System Model).

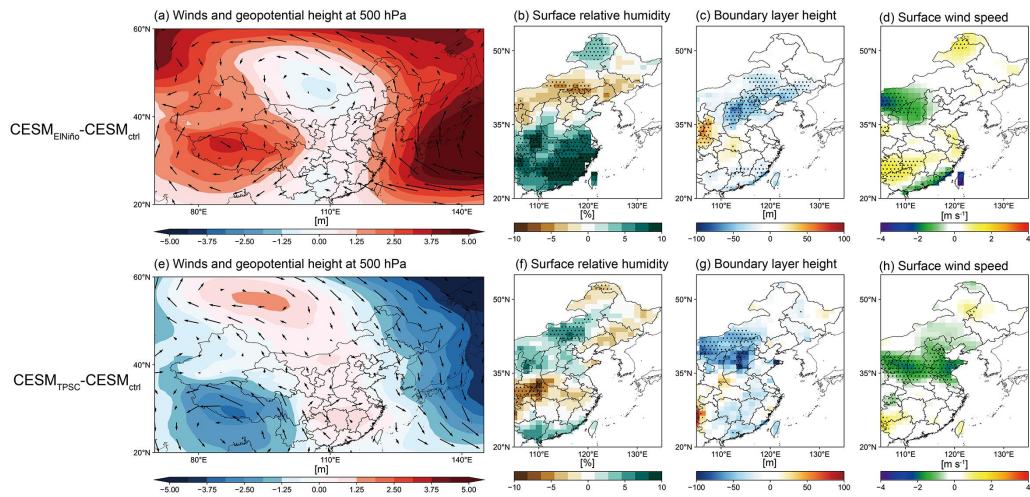


Figure S6. CESM simulated responses of (a, e) geopotential height (m, contour) and wind fields (m s^{-1} , vector) at 500 hPa, (b, f) surface relative humidity (%), (c, g) planetary boundary layer height (m) and (d, h) surface wind speed (m s^{-1}) during winter to Niño 1+2, and higher albedo forcing over the northern TP. Dotted areas indicate responses that are significant at the 95% confidence level based on a two-tailed Student's *t* test applied to daily simulated anomalies during the winter period.

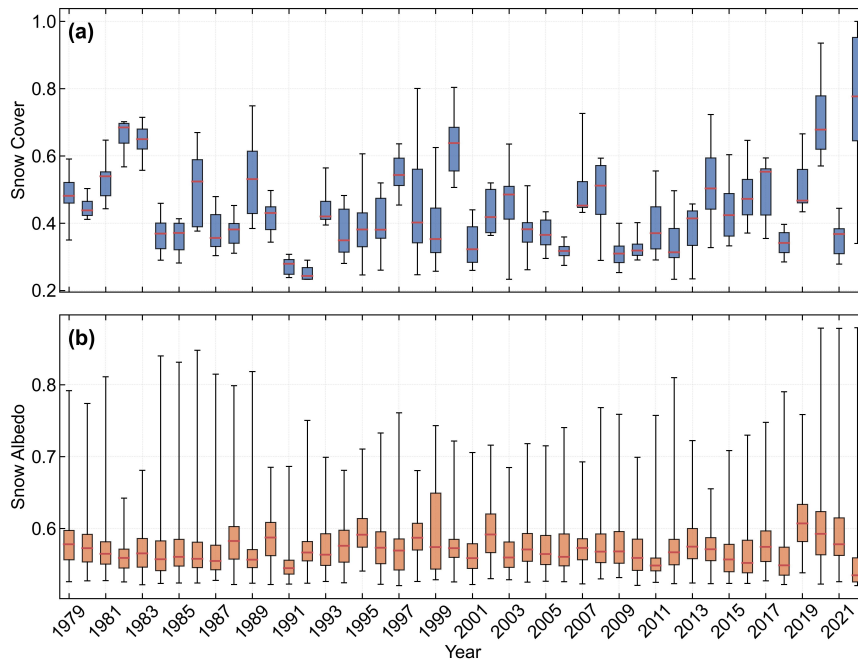


Figure S7. Interannual variations in winter (a) snow cover extent and (b) snow albedo over the northern Tibetan Plateau (86°-94°E, 35°-40°N) during 1979-2021. In each boxplot, the central red line denotes the median value, the box boundaries indicate the interquartile range (25th-75th percentiles), and the whiskers represent the minimum and maximum values.